Published by Institute of Physics Publishing for SISSA/ISAS

Received: *February 8, 2002*
Revised: *March 18, 2002*
Accepted: *March 19, 2002*

Neutralino relic density in minimal supergravity with co-annihilations

Howard Baer, Csaba Balázs and Alexander Belyaev

Department of Physics, Florida State University
Tallahassee, FL, USA 32306
E-mail: baer@hep.fsu.edu, balazs@hep.fsu.edu, belyaev@hep.fsu.edu

Abstract: We evaluate the relic density of neutralinos in the minimal supergravity (mSUGRA) model. All $2 \to 2$ neutralino annihilation diagrams, as well as all processes involving sleptons, charginos , neutralinos and third generation squarks are included. Relativistic thermal averaging of the velocity times cross sections is performed. We find that co-annihilation effects are only important on the edges of the model parameter space, where some amount of fine-tuning is necessary to obtain a reasonable relic density. Alternatively, at high $\tan\beta$, annihilation through very broad Higgs resonances gives rise to an acceptable neutralino relic density over broad regions of parameter space where little or no fine-tuning is needed. Finally, we compare our results against the reach of various e^+e^- and hadron colliders for supersymmetric matter.

Keywords: Dark Matter, Supersymmetric Standard Model.

Contents

1. Introduction

A wide variety of astrophysical measurements are being used to pin down some of the basic cosmological parameters of the universe. High resolution maps of the cosmic microwave background (CMB) radiation [1] imply that the energy density of the universe $\Omega = \rho/\rho_c \simeq 1$, consistent with inflationary cosmology. Here, $\rho_c = 3H^2/8\pi G_N$ is the critical closure density of the universe, where G_N is Newton's constant and $H = 100h$ km/sec/Mpc is the scaled Hubble constant. The value of h itself is determined to be $\sim 0.7 \pm 0.1$ by improved measurements of distant galaxies [2]. Meanwhile, data from distant supernovae [3] imply a nonzero dark energy content of the universe $\Omega_\Lambda \sim 0.7$, a result which is confirmed by fits to the CMB power spectrum [4]. Analyses of Big Bang nucleosynthesis [5] imply the baryonic density $\Omega_b h^2 \simeq 0.020 \pm 0.002$, although the CMB fits suggest a somewhat higher value of ~ 0.03. Hot dark matter, for instance from massive neutrinos, should give only a small contribution to the total matter density of the universe. In contrast, a variety of data ranging from galactic rotation curves to large scale structure and the CMB imply a significant density of cold dark matter (CDM) [6] $\Omega_c h^2 \simeq 0.2 \pm 0.1$.

In many R-parity conserving supersymmetric models of particle physics, the lightest neutralino ($\widetilde{Z}_1$) is also the lightest SUSY particle (LSP); as such, it is massive, neutral and stable. For this case, relic neutralinos left over from the Big Bang provide an excellent candidate for the CDM content of the universe [7]. In the early universe, such neutralinos would exist in thermal equilibrium with the cosmic soup. As the universe expanded and cooled, the thermal energy would no longer be sufficient to produce neutralinos at an appreciable rate, although they could still annihilate away. Their number density is governed by the Boltzmann equation formulated for a Friedmann-Robertson-Walker universe.

In this paper, our goal is to present results of calculations of the neutralino relic density within the context of the paradigm minimal supergravity model (mSUGRA, or CMSSM) [8]. In mSUGRA, it is assumed that SUSY breaking occurs in a hidden sector of the model, with SUSY breaking effects communicated from hidden to observable sectors via gravitational interactions. The model parameter space is given by

$$m_0,\ m_{1/2}\,, \qquad A_0\,, \qquad \tan\beta \quad \text{and} \quad \text{sign}(\mu)\,. \tag{1.1}$$

Here, m_0 is the universal scalar mass, $m_{1/2}$ is the universal gaugino mass and A_0 is the universal trilinear mass all evaluated at M_{GUT}, while $\tan\beta$ is the ratio of Higgs field vevs (v_u/v_d), and μ is a supersymmetric Higgs mass term. The soft SUSY breaking parameters, along with gauge and Yukawa couplings, evolve from M_{GUT} to $M_{\rm weak}$ according to their renormalization group (RG) equations. At $M_{\rm weak}$, the RG improved 1-loop effective potential is minimized, and electroweak gauge symmetry is broken radiatively. In this report, we implement the mSUGRA solution encoded in ISAJET v7.59 [9].

There is a long history of increasingly sophisticated solutions for the relic density of neutralinos in supersymmetric models [10]–[32]. The key ingredient to solving the Boltzmann equation is to evaluate the thermally averaged neutralino annihilation cross section times velocity factor. Traditionally, the solution is made by expanding the annihilation cross section as a power series in neutralino velocity, so that angular and energy integrals can be evaluated analytically. The remaining integral over temperature can then be performed numerically. The power series solution is excellent in many regions of model parameter space because the relic neutralino velocity is expected to be highly non-relativistic.

However, it was emphasized by Griest and Seckel that annihilations may occur through s-channel resonances at high enough energies [14] that a relativistic treatment of thermal averaging might be necessary. Drees and Nojiri found that at large values of the parameter $\tan\beta$, neutralino annihilation can be dominated by s-channel scattering through very broad A and H Higgs resonances [17]. The proper formalism for relativistic thermal averaging was developed by Gondolo and Gelmini (GG) [15], and was implemented in the code of Baer and Brhlik [20, 22]. Working within the framework of the mSUGRA model, it was found [20, 22, 23, 29, 30] that at large $\tan\beta$, indeed large new regions of model parameter space gave rise to reasonable values for the CDM relic density. At large $\tan\beta$, the A and H resonances are broad enough (typically 10-50 GeV¡) that even if the quantity $2m_{\widetilde{Z}_1}$ is several partial widths away from exact resonance, there can still be a significant rate for neutralino annihilation. Thus, in the mSUGRA model at low m_0 and $\tan\beta$, neutralino annihilation is dominated by t-channel slepton exchange, and reasonable values of the relic density occur only for relatively low values of m_0 and $m_{1/2}$. At high $\tan\beta$, a much larger parameter space is allowed, owing to off-resonance neutralino annihilation through the broad Higgs resonances.

In addition, there exist regions of mSUGRA model parameter space where co-annihilation processes are important, and even dominant. It was stressed by Griest and Seckel [14] that in regions with a higgsino-like LSP, the $\widetilde{Z}_1$, $\widetilde{W}_1$ and $\widetilde{Z}_2$ masses become nearly degenerate, so that all three species can exist in thermal equilibrium, and annihilate against one another. The relativistic thermal averaging formalism of GG was extended to include co-annihilation processes by Edsjö and Gondolo [21], and was implemented in the DarkSUSY code [24] for co-annihilation of charginos and heavier neutralinos.

JHEP03(2002)042

The importance of neutralino-slepton co-annihilation was stressed by Ellis *et al.* and others [26]–[30]. In regions of mSUGRA parameter space where $\widetilde{Z}_1$ and $\tilde{\tau}_1$ (or other sleptons) were nearly degenerate (at low m_0), co-annihilations could give rise to reasonable values of the relic density even at very large values of $m_{1/2}$, at both low and high $\tan\beta$. In addition, for large values of the parameter A_0 or for non-universal scalar masses, top or bottom squark masses could become nearly degenerate with the $\widetilde{Z}_1$, so that squark co-annihilation processes can become important as well [31, 32].

In this paper, our goal is to calculate the relic density of neutralinos in the mSUGRA model including co-annihilation processes in addition to *relativistic* thermal averaging of the annihilation cross section times velocity. Since there are very many Feynman diagrams to evaluate for neutralino annihilations and co-annihilations, we use CompHEP v.33.24 [33], which provides for fast and efficient automatic evaluation of tree level processes in the SM or MSSM. For initial states including $\widetilde{Z}_1$, $\widetilde{Z}_2$, $\widetilde{W}_1$, $\tilde{e}_1$, $\tilde{\mu}_1$, $\tilde{\tau}_1$, $\tilde{t}_1$ and $\tilde{b}_1$, we count 1722 subprocesses, including 7618 Feynman diagrams. For those processes we have calculated the squared matrix element and have written it down in the form of CompHEP FORTRAN output.

The weak scale parameters from supersymmetric models are generated using ISAJET v7.59, and interfaced with the squared matrix elements from CompHEP. Details of our computational algorithm are given in section 2. In section 3 we present a variety of results for the relic density in mSUGRA model parameter space. Much of parameter space is ruled out at low $\tan\beta$ since the relic density is too high, and would yield too small an age of the universe. At high $\tan\beta$, large regions of parameter space are available with a reasonable relic density in the range $0.1 < \Omega_{\widetilde{Z}_1} h^2 < 0.3$. In section 4, we compare our results with some previous results on the reach of colliders, and draw some implications. In section 5, we conclude.

As we were completing this work, the group of Belanger, Boudjema, Pukhov and Semenov reported on a calculation similar to ours in scope and method [34]. In addition, a paper by Nihei, Roszkowski and de Austri appeared, containing analytic calculations of all $\widetilde{Z}_1\widetilde{Z}_1$ annihilation cross sections [35].

2. Calculational details

The evolution of the number density of supersymmetric relics in the universe is described by the Boltzmann equation as formulated for a Friedmann-Robertson-Walker universe. For calculations including many particle species, such as the case where co-annihilations are important, there is a Boltzmann equation for each particle species. Following Griest and Seckel [14], the equations can be combined to obtain a single equation

$$\frac{dn}{dt} = -3Hn - \langle\sigma_{\text{eff}} v\rangle \left(n^2 - n_{\text{eq}}^2\right), \tag{2.1}$$

where

$$n = \sum_{i=1}^{N} n_i \tag{2.2}$$

and the sum extends over the N particle species contributing to the relic density, with n_i being the number density of the ith species. Furthermore, $n_{eq,i}$ is the number density of the ith species in thermal equilibrium, given by

$$n_{\mathrm{eq},i} = \frac{g_i m_i^2 T}{2\pi^2} K_2\left(\frac{m_i}{T}\right), \tag{2.3}$$

where K_j is a modified Bessel function of the second kind of order j.

The quantity $\langle\sigma_{\mathrm{eff}} v\rangle$ is the thermally averaged cross section times velocity. A succinct expression for this quantity using relativistic thermal averaging was computed by Gondolo and Gelmini for the case of a single particle species [15], and was extended by Edsjö and Gondolo for the case including co-annihilations [21]. We adopt this latter form, given by

$$\langle\sigma_{\mathrm{eff}} v\rangle(x) = \frac{\int_2^\infty K_1\left(\frac{a}{x}\right)\sum_{i,j=1}^N \lambda(a^2, b_i^2, b_j^2) g_i g_j \sigma_{ij}(a) da}{4x\left(\sum_{i=1}^N K_2(b_i/x)\, b_i^2 g_i\right)^2}, \tag{2.4}$$

where $x = T/m_{\widetilde{Z}_1}$ is the temperature in units of mass of the relic neutralino, σ_{ij} is the cross section for the annihilation reaction $ij \to X$ (X is any allowed final state consisting of 2 SM and/or Higgs particles), $\lambda(a^2, b_i^2, b_j^2) = a^4 + b_i^4 + b_j^4 - 2(a^2 b_i^2 + a^2 b_j^2 + b_i^2 b_j^2)$, $a = \sqrt{s}/m_{\widetilde{Z}_1}$ and $b_i = m_i/m_{\widetilde{Z}_1}$. This expression is our master formula for the relativistically thermal averaged annihilation cross section times velocity.

To solve the Boltzmann equation, we introduce a freeze-out temperature T_F, so that the relic density of neutralinos is given by[1]

$$\Omega_{\widetilde{Z}_1} h^2 = \frac{\rho(T_0)}{8.1\times 10^{-47}\,\mathrm{GeV}^4}, \tag{2.5}$$

where

$$\rho(T_0) \simeq 1.66 \frac{1}{M_{Pl}}\left(\frac{T_{m_{\widetilde{Z}_1}}}{T_\gamma}\right)^3 T_\gamma^3 \sqrt{g_*}\frac{1}{\int_0^{x_F}\langle\sigma_{\mathrm{eff}} v\rangle dx}. \tag{2.6}$$

The freeze-out temperature $x_F = T_F/m_{\widetilde{Z}_1}$ is determined as usual by an iterative solution of the freeze-out relation

$$x_F^{-1} = \log\left[\frac{m_{\widetilde{Z}_1}}{2\pi^3}\frac{g_{\mathrm{eff}}}{2}\sqrt{\frac{45}{2g_* G_N}}\langle\sigma_{\mathrm{eff}} v\rangle(x_F)\, x_F^{1/2}\right]. \tag{2.7}$$

Here, g_{eff} denotes the effective number of degrees of freedom of the co-annihilating particles, as defined by Griest and Seckel [14]. The quantity g_* is the SM effective degrees of freedom parameter with $\sqrt{g_*} \simeq 9$ over our region of interest.

The challenge then is to evaluate all possible channels for neutralino annihilation to SM and/or Higgs particles, and also all co-annihilation reactions. The 7618 Feynman diagrams are evaluated using CompHEP, leading to about 50 MB of FORTRAN code. To achieve our final result with relativistic thermal averaging, a three-dimensional integral must be performed over i.) the final state subprocess scattering angle θ, ii.) the subprocess energy

[1] The procedure we follow gives numerical results valid to about 10% versus a direct numerical solution of the Boltzmann equation [15].

parameter $a = \sqrt{s}/m_{\widetilde{Z}_1}$, and iii.) the temperature T from freeze-out T_F to the present day temperature of the universe, which can effectively be taken to be 0. We perform the three-dimensional integral using the BASES algorithm [36], which implements sequentially improved sampling in multi-dimensional Monte Carlo integration, generally with good convergence properties. We note that the three-dimensional integration appearing in the case of our relativistic calculations involving several species in thermal equilibrium is about 2 orders of magnitude more CPU-time consuming than the series expansion approach, which requires just one numerical integration.

3. Results

Our first results in figure 1 show regions of $\Omega_{\widetilde{Z}_1}h^2$ in the m_0 vs. $m_{1/2}$ plane in the minimal supergravity model for $A_0 = 0$, $\tan\beta = 10$ and for $\mu < 0$ and $\mu > 0$. The upper plots show the contribution if only $\widetilde{Z}_1\widetilde{Z}_1$ annihilation reactions occur, while the lower frames include as well all co-annihilation processes. The red shaded regions are excluded by theoretical constraints (lack of REWSB on the right, a charged LSP in the upper left). The unshaded regions have $\Omega_{\widetilde{Z}_1}h^2 > 1$, and should be excluded, as they would lead to a universe of age less than 10 billion years, in conflict with the oldest stars found in globular clusters. The light blue shaded regions have $\Omega_{\widetilde{Z}_1}h^2 < 0.02$, which wouldn't be enough CDM even to explain galactic rotation curves. The green region yields values of $0.1 < \Omega_{\widetilde{Z}_1}h^2 < 0.3$, i.e. in the most cosmologically favored region. The yellow ($0.02 < \Omega_{\widetilde{Z}_1}h^2 < 0.1$) and dark blue ($0.3 < \Omega_{\widetilde{Z}_1}h^2 < 1$) correspond to regions with intermediate values of low and high relic density, respectively. Points with $m_{1/2} \lesssim 150\,\text{GeV}$ give rise to chargino masses below bounds from LEP2; the LEP2 excluded regions due to chargino, slepton and Higgs searches are not shown on these plots, but will be shown in section 4.

The structure of these plots can be understood by examining the thermally averaged cross section times velocity, integrated from zero temperature to T_F. In figure 2 we show this quantity for a variety of contributing subprocesses plotted versus m_0 for fixed $m_{1/2} = 300\,\text{GeV}$, $\mu > 0$, and all other parameters as in figure 1. At low values of m_0, the neutralino annihilation cross section is dominated by t-channel scattering into leptons pairs, as shown by the black solid curve. However, at the very lowest values of m_0, the annihilation rate is sharply increased by neutralino-stau and stau-stau co-annihilations, leading to very low relic densities where $m_{\widetilde{Z}_1} \simeq m_{\tilde{\tau}_1}$ [26]. As m_0 increases, the slepton masses also increase, which suppresses the annihilation cross section, and the relic density rises to values $\Omega_{\widetilde{Z}_1}h^2 > 1$. When m_0 increases further, to beyond the $\sim 1\,\text{TeV}$ level, and approaches the excluded region, the magnitude of the μ parameter falls, and the higgsino component of $\widetilde{Z}_1$ increases. This is the so called "focus point" region, explored in ref. [25]. In this region, the annihilation rate is dominated by scattering into WW, ZZ and Zh channels. At even higher m_0 values, $m_{\widetilde{Z}_1} \simeq m_{\widetilde{W}_1} \simeq m_{\widetilde{Z}_2}$, and these co-annihilation channels increase even more the annihilation rate. Finally, at the large m_0 bound on parameter space, $|\mu| \to 0$, and appropriate REWSB no longer occurs. Most of the structure of figure 1 can be understood in these terms, with the exception being the horizontal band of very low relic density at $m_{1/2} \simeq 125\,\text{GeV}$.

JHEP03(2002)042

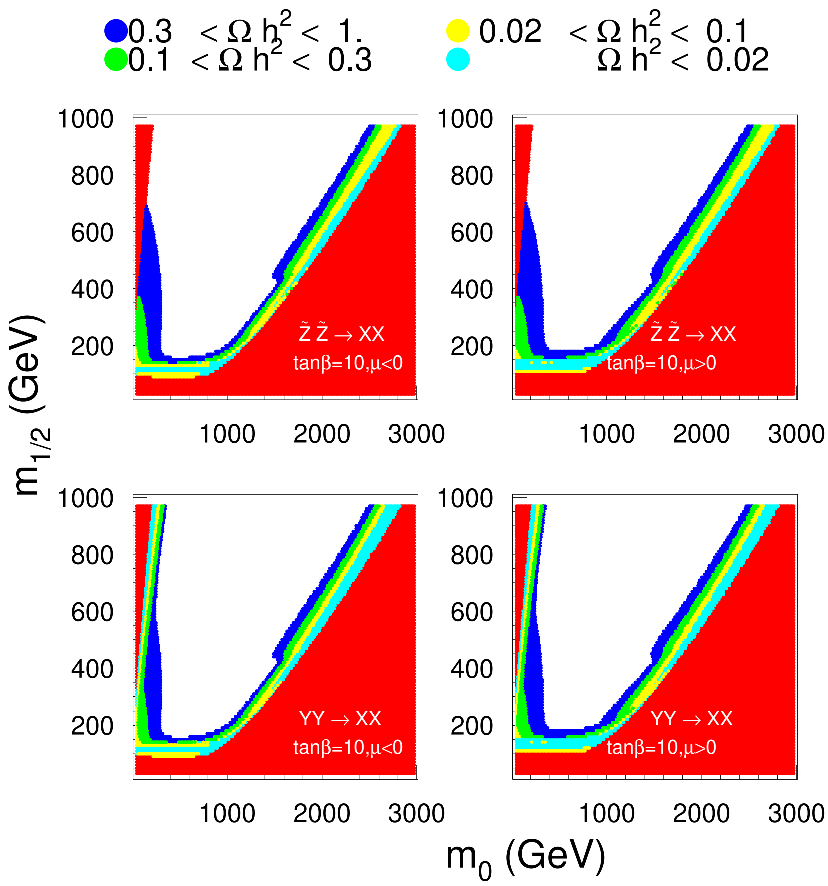

Figure 1: Regions of neutralino relic density in the m_0 vs. $m_{1/2}$ plane for $A_0 = 0$ and $\tan\beta = 10$. The upper two frames show the contribution for only $\widetilde{Z}_1\widetilde{Z}_1$ annihilation, while the lower frames include as well all co-annihilation processes.

In this region, which is nearly excluded by LEP2 bounds on the chargino mass, there is enhanced neutralino annihilation through the Z and h resonances. In fact, a higher degree of resolution on our plots would resolve these horizontal bands into *two* bands, corresponding to each of the separate resonances, as shown in ref. [20]. Finally, the glitch in contours around $m_0 \sim 1500\,\text{GeV}$ and $m_{1/2} \sim 425\,\text{GeV}$ occurs because $m_{\widetilde{Z}_1} \simeq m_t = 175\,\text{GeV}$, so that $\sigma(\widetilde{Z}_1\widetilde{Z}_1 \to t\bar{t})$ becomes large.

The m_0 vs. $m_{1/2}$ planes for $\tan\beta = 30$ are shown in figure 3. The structure of these plots are qualitatively the same as in figure 1. Quantitatively, they differ mainly in that the cosmologically favored regions are expanding as $\tan\beta$ grows. One reason is that the light stau becomes even lighter as $\tan\beta$ increases, and this increases the neutralino annihilation rate $\widetilde{Z}_1\widetilde{Z}_1 \to \tau\bar{\tau}$ through t-channel stau exchange. In addition, the bottom and tau Yukawa couplings increase with $\tan\beta$, which increases the annihilation cross sections into τs and bs. Finally, the H and A Higgs boson masses are decreasing with $\tan\beta$, and annihilation rates which proceed through these resonances increase. Co-annihilations again gives enhanced annihilation cross sections on the left and farthest right hand sides of the allowed parameter space.

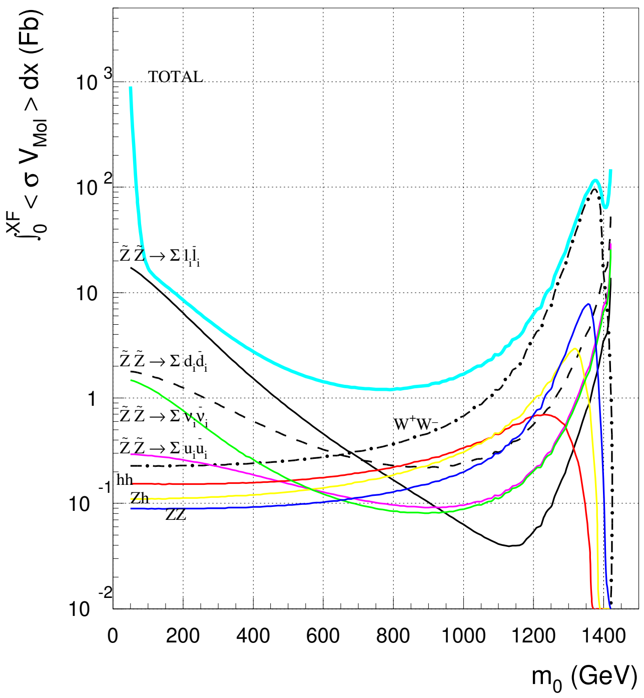

Figure 2: Thermally averaged cross section times velocity integrated from $T = 0$ to T_F, for various component subprocess cross sections. The blue curve denotes the total of all annihilation and co-annihilation reactions. We show results versus m_0 for $m_{1/2} = 300\,\text{GeV}$, $\mu > 0$, $A_0 = 0$ and $\tan\beta = 10$.

In figure 4, we show the m_0 vs. $m_{1/2}$ plane for $\tan\beta = 45$. In this case, the structure of the plane is changing qualitatively, especially for $\mu < 0$. First, there is a new region of disallowed parameter space for $\mu < 0$ in the lower left due to $m_A^2 < 0$, which signals a breakdown of the REWSB mechanism. Second, a corridor of very low relic density passes diagonally through the plot. The center of this region is where $2m_{\widetilde{Z}_1} \simeq m_A$ and m_H. At the A and H resonance, there is very efficient neutralino annihilation into $b\bar{b}$ final states. This is illustrated in figure 5, where we show the integrated annihilation cross section times velocity versus m_0 for $m_{1/2} = 600\,\text{GeV}$ and $\mu < 0$. At the very lowest values of m_0, there is again the sharp peak due to neutralino-stau and stau-stau co-annihilations. For larger values of m_0, however, the annihilation rate is dominantly into $b\bar{b}$ final states over almost the entire m_0 range. This is due to the large annihilation rates through the s-channel A and H diagrams, even when the reactions occur off resonance. In this case, the widths of the A and H are so large (both $\sim 10-40\,\text{GeV}$ across the range in m_0 shown) that efficient s-channel annihilation can occur throughout the bulk of parameter space, even when the resonance condition is not exactly fulfilled. The resonance annihilation is explicitly displayed in this plot as the annihilation bump at m_0 just below $1300\,\text{GeV}$. Another annihilation possibility is that $\widetilde{Z}_1\widetilde{Z}_1 \to b\bar{b}$ via t and u channel graphs. In fact, these annihilation graphs are enhanced due to the large b Yukawa coupling and decreasing value of $m_{\tilde{b}_1}$, but we have checked that the s-channel annihilation is still far the dominant channel. Annihilation into $\tau\bar{\tau}$ is the next most likely channel, but is always below the level

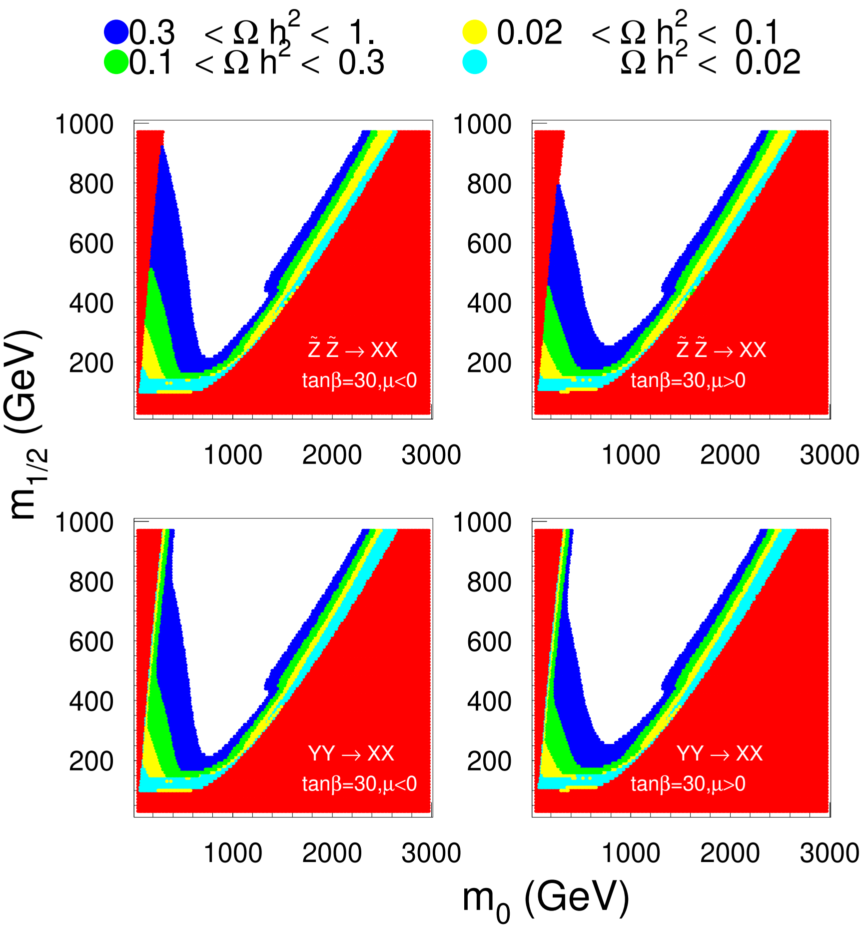

Figure 3: Regions of neutralino relic density in the m_0 vs. $m_{1/2}$ plane for $A_0 = 0$ and $\tan\beta = 30$. The upper two frames show the contribution for only $\widetilde{Z}_1\widetilde{Z}_1$ annihilation, while the lower frames include as well all co-annihilation processes.

of annihilation into $b\bar{b}$ for the parameters shown in figure 5. At even higher values of m_0 where the higgsino component of $\widetilde{Z}_1$ becomes non-negligible, the annihilations into WW and ZZ again dominate; finally, at the highest values of m_0, the $\widetilde{W}_1$ and $\widetilde{Z}_2$ co-annihilation channels become important.

In figure 6, we show again the subprocess annihilation rates versus m_0 for $\tan\beta = 45$, but this time for $\mu > 0$ and for $m_{1/2} = 300\,\mathrm{GeV}$. Although no explicit resonance is evident for $\mu > 0$, the dominant annihilations are once again into $b\bar{b}$ final states over most of the parameter space, due to the very wide Higgs resonances. At the highest values of m_0, where μ is becoming small, the annihilation rate into the dominant WW and ZZ final states becomes suppressed. The suppression is due to the diminishing mass of the $\widetilde{Z}_1$ as $\mu \to 0$. As $m_{\widetilde{Z}_1}$ falls below M_Z and then M_W, there is thermal suppression of annihilation into the ZZ and WW final states.

To summarize the regions of mSUGRA model parameter space with reasonable values of neutralino relic density, we can label four important regions: i.) annihilation through t-channel slepton– especially stau– exchange, as occurs for low values of m_0 and $m_{1/2}$, ii.)

JHEP03(2002)042

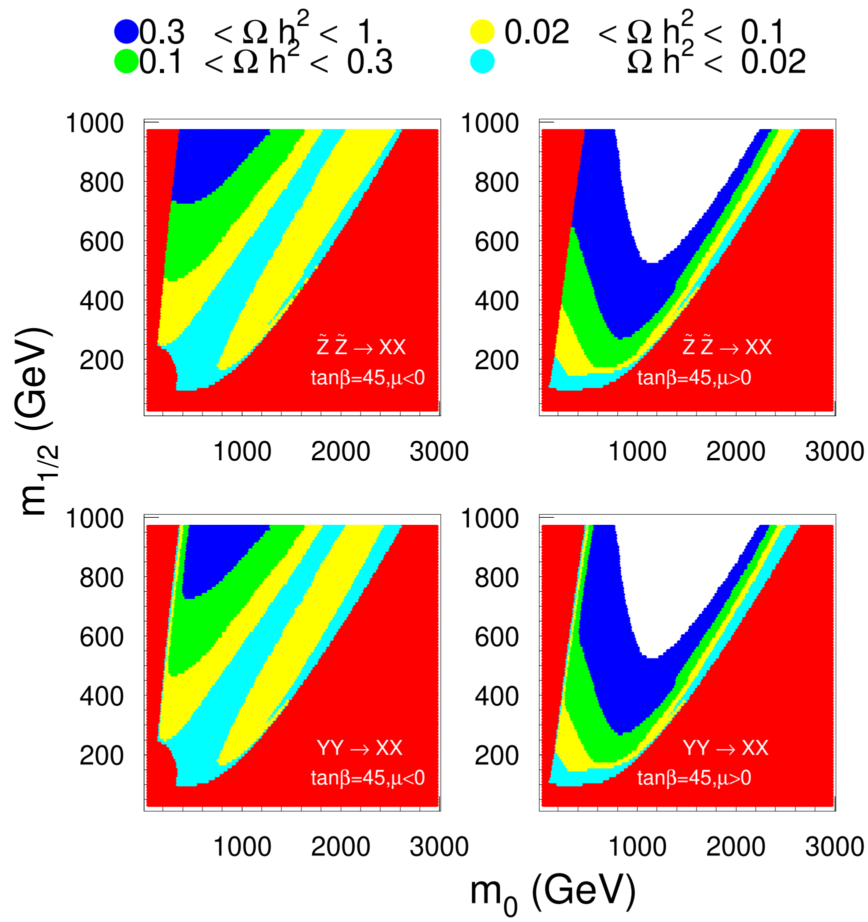

Figure 4: Regions of neutralino relic density in the m_0 vs. $m_{1/2}$ plane for $A_0 = 0$ and $\tan\beta = 45$. The upper two frames show the contribution for only $\widetilde{Z}_1\widetilde{Z}_1$ annihilation, while the lower frames include as well all co-annihilation processes.

the stau co-annihilation region for low values of m_0 on the edge of the excluded region, iii.) the large m_0 region with non-negligible higgsino-component annihilation, and also $\widetilde{W}_1$ (and possibly $\widetilde{Z}_2$) co-annihilation occurs near the edge of the limit of parameter space, and *iv.*) annihilation into $b\bar{b}$ and $\tau\bar{\tau}$ final states through s-channel A and H resonances at high $\tan\beta$. Other regions can include top or bottom squark co-annihilation for large values of A_0, again on the edge of parameter space where $\tilde{t}_1$ or $\tilde{b}_1$ become light, or annihilation through Z or h resonances. These latter regions are essentially excluded now by constraints on sparticle masses from LEP2.

It is useful to view the relic density $\Omega_{\widetilde{Z}_1}h^2$ directly as a function of model parameters. We show in figure 7 the value of $\Omega_{\widetilde{Z}_1}h^2$ versus the parameter m_0 for fixed $m_{1/2} = 600\,\mathrm{GeV}$, $A_0 = 0$, $\mu < 0$ and for $\tan\beta = 10$, 30 and 45. The dashed curves show the result with no co-annihilations, while the solid curves yield the complete calculation. The shaded band denotes the cosmologically favored region with $0.1 < \Omega_{\widetilde{Z}_1}h^2 < 0.3$. For this value of $m_{1/2}$, the lower $\tan\beta$ curves yield a favored relic density only in the very low and very high m_0 regions, and here the curves have a very sharp slope. The large slope is indicative of large

JHEP03(2002)042

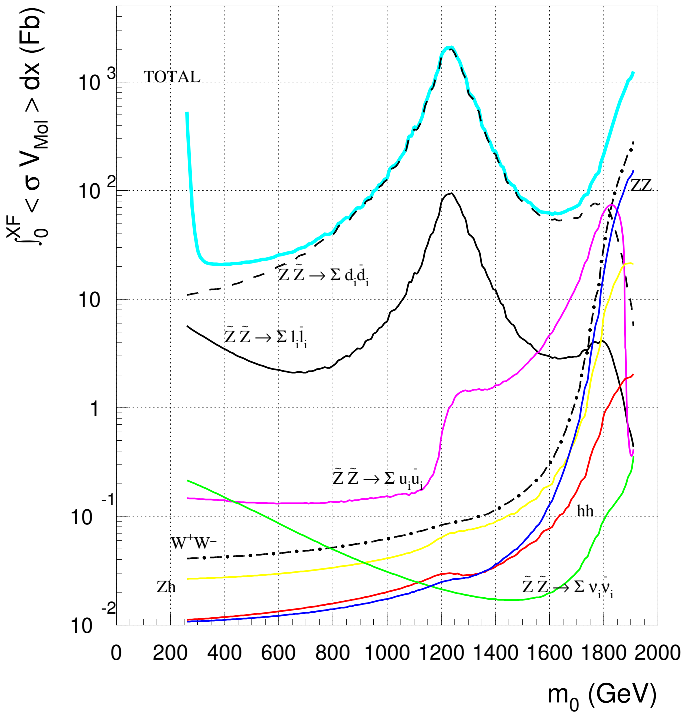

Figure 5: Thermally averaged cross section times velocity evaluated at T_F for various component subprocess cross sections. The blue curve denotes the total of all annihilation and co-annihilation reactions. We show results versus m_0 for $m_{1/2} = 600\,\mathrm{GeV}$, $\mu < 0$, $A_0 = 0$ and $\tan\beta = 45$.

fine-tuning, in that a small change of model parameters, in this case m_0, yields a large change in $\Omega_{\widetilde{Z}_1} h^2$. In contrast, the $\tan\beta = 45$ curve shows a large region with good relic density and nearly zero slope, hence very little fine-tuning.

In figure 8, we show the corresponding values of the fine-tuning, basically the logarithmic derivative, as advocated by Ellis and Olive [37]:

$$\Delta(m_0) = \left| \frac{m_0}{\Omega_{\widetilde{Z}_1} h^2} \frac{\partial \Omega_{\widetilde{Z}_1} h^2}{\partial m_0} \right| . \tag{3.1}$$

As indicated earlier, the low fine-tuning regions mostly coincide with that of neutralino annihilation via t-channel slepton exchange (region i.)), or off-resonance annihilation through A and H (region iv.)). The co-annihilation region ii.) and focus point region iii.) tend to have higher fine-tunings due to the steep rise of the cross sections. Regions with simultaneous low fine-tuning and preferred $\Omega_{\widetilde{Z}_1} h^2$ values are the best candidates for viable mSUGRA parameters.

In figure 9, we show $\Omega_{\widetilde{Z}_1} h^2$ versus m_0 for $m_{1/2} = 300\,\mathrm{GeV}$, $A_0 = 0$, $\mu > 0$ and the same three $\tan\beta$ parameters. The curves reflect the broad regions of parameter space with reasonable relic density values at high $\tan\beta$. The corresponding plot of the fine-tuning parameter is shown in figure 10. Again, there is large fine-tuning at the edges of parameter space, but low fine-tuning in the intermediate regions. In conclusion, the relic density and the fine-tuning parameter together tend to prefer mSUGRA model parameters in regions

JHEP03(2002)042

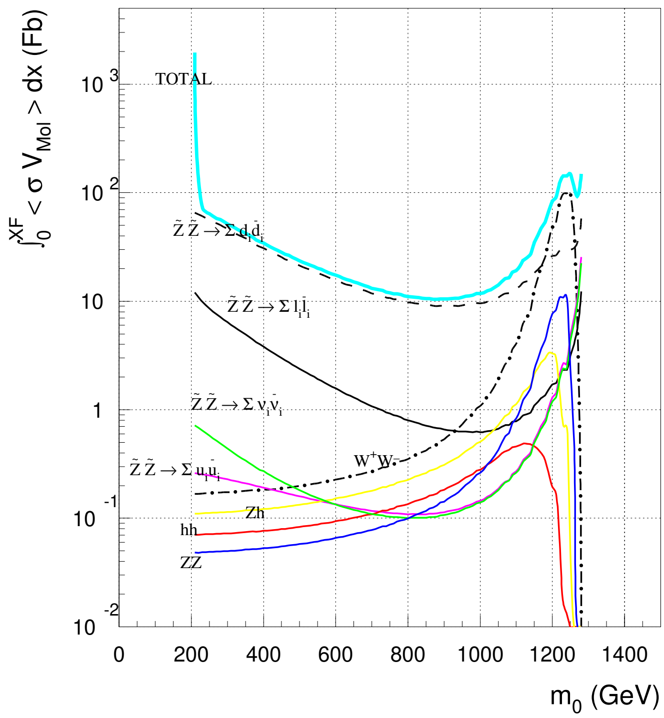

Figure 6: Thermally averaged cross section times velocity evaluated at T_F for various component subprocess cross sections. The blue curve denotes the total of all annihilation and co-annihilation reactions. We show results versus m_0 for $m_{1/2} = 300\,\text{GeV}$, $\mu > 0$, $A_0 = 0$ and $\tan\beta = 45$.

i.) or iv.). These two regions lead to distinct collider signatures for future searches for supersymmetric matter.

4. Comparison with collider reaches

It is worthwhile to compare our results on the neutralino relic density with various collider reaches[2]. To do so, we first show in figure 11 the m_0 vs. $m_{1/2}$ plane for $\tan\beta = 10$, $A_0 = 0$ and $\mu > 0$, but this time including information from different collider projections. First, the region excluded by LEP2 sparticle searches is shown by the pink shading, and reflects mSUGRA model points where $m_{\widetilde{W}_1} < 100\,\text{GeV}$, $m_{\tilde{e}_1} < 100\,\text{GeV}$, or $m_{\tilde{\tau}_1} < 76\,\text{GeV}$ [38]. These LEP2 bounds sharply constrain the regions where neutralino annihilation could occur via the Z and light Higgs h resonances. In addition, we plot contours of light Higgs boson mass $m_h = 110$, 115 and 120 GeV. Since the light Higgs scalar h is usually SM-like in the mSUGRA model, the region below $m_h = 115\,\text{GeV}$ is largely excluded [39] by the direct LEP2 Higgs search. We note that the Higgs mass varies slowly in parameter space, so a small change in Higgs mass can lead to large changes in model parameters. Thus, these bounds may have some fuzziness to them, reflecting uncertainties on the theoretical calculations and experimental search results. The reach of the Fermilab Tevatron for SUSY

[2]Non-accelerator direct and indirect dark matter search reach results are summarized in the last two papers of ref. [25]

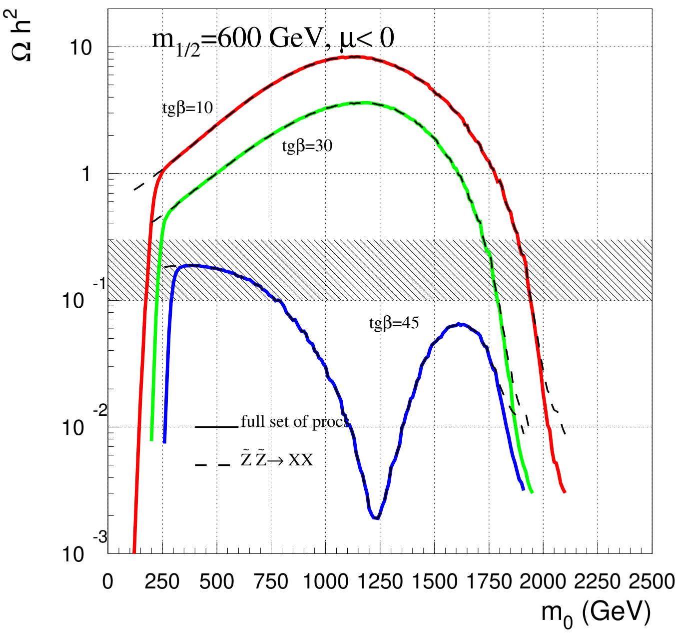

Figure 7: Neutralino relic density $\Omega_{\widetilde{Z}_1}h^2$ versus m_0 for $m_{1/2} = 600$, $A_0 = 0$, $\mu < 0$ and $\tan\beta = 10$, 30 and 45. The shaded region denotes the cosmologically favored values of $\Omega_{\widetilde{Z}_1}h^2$.

particles has been estimated recently in ref. [40] for an integrated luminosity of 25 fb^{-1}. Almost all the reach comes from the search for clean trilepton events. The 3σ reach is denoted by the two lower black contours. The results show that Tevatron experiments will be able to probe a significant part of the favored relic density region where annihilation occurs through t-channel slepton exchange. Also, some of the "focus point" region [41] with large m_0 and small $m_{1/2}$ is accessible.

The reach of the CERN LHC is also shown for 10 fb^{-1} of integrated luminosity [42]. The LHC reach extends well beyond the t-channel slepton region, but cannot exclude all the low and high m_0 regions corresponding to slepton co-annihilations or to higgsino-like neutralinos, where annihilation cross sections are enhanced. We remark, however, that these regions on the edge of parameter space, although perhaps not directly accessible to LHC searches, are also disfavored by fine-tuning requirements.

We also show the reach of a linear e^+e^- collider for SUSY particles for $\sqrt{s} = 500$ GeV (NLC500) and $\sqrt{s} = 1000$ GeV (NLC1000), assuming 30 fb^{-1} of integrated luminosity [43]. The left-most NLC region is explorable via slepton pair searches, while the lower and right NLC regions are explorable via chargino pair searches. A small intermediate region is accessible via $e^+e^- \to \widetilde{Z}_1\widetilde{Z}_2$ searches.

A similar comparison of neutralino relic density versus collider searches is shown in figure 12, although in this case, results for the NLC reach are unavailable. A large part of the green region is actually excluded by the LEP2 Higgs search results. Furthermore, the reach of the Fermilab Tevatron barely extends to the cosmologically favored region. The CERN LHC covers most of the green region, with the exception of the stau co-annihilation band, and the higgsino-like LSP band.

JHEP03(2002)042

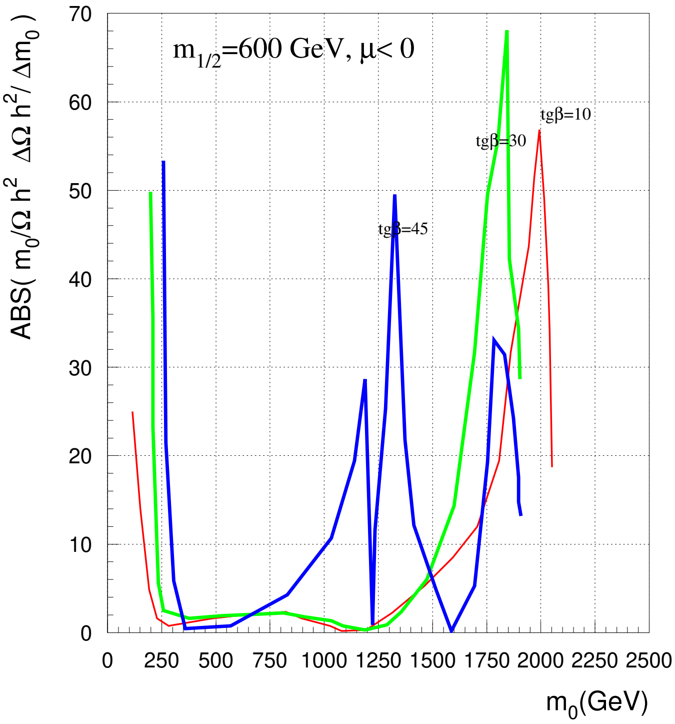

Figure 8: The fine tuning parameter as the function of m_0 for $\tan\beta = 10, 30, 45$ and for the parameter slice $m_{1/2} = 600\,\mathrm{GeV}$, $\mu < 0$.

5. Conclusions

In conclusion, we have performed a calculation of the neutralino relic density in the minimal supergravity model including all $2 \to 2$ neutralino annihilation and co-annihilation processes, where the initial state includes $\widetilde{Z}_1$, $\widetilde{Z}_2$, $\widetilde{W}_1$, $\tilde{e}_1$, $\tilde{\mu}_1$, $\tilde{\tau}_1$, $\tilde{t}_1$ and $\tilde{b}_1$. The calculation was performed using the CompHEP program for automatic evaluation of Feynman diagrams, coupled with ISAJET for sparticle mass evaluation in the mSUGRA model, and for standard and supersymmetric couplings and decay widths. We implemented relativistic thermal averaging, which is especially important for evaluating the relic density when resonances in the annihilation cross section are present, and neutralino thermal velocities can be relativistic. The three-dimensional integration was performed by Monte Carlo evaluation with importance sampling, which yields in general good convergence even in the presence of narrow resonances. We note once again that a calculation of similar scope and procedure was recently reported in ref. [34].

It may be useful to compare our results against other recent evaluations of the neutralino relic density including all co-annihilation effects. We compared against several recently published results [26, 23, 29, 30]. Our results agree qualitatively with these other published results. Quantitatively, these various papers largely disagree amongst themselves and with our work at very large values of $\tan\beta$. In this region, even one loop calculations of sparticle and Higgs boson masses can be very unstable, and especially the value of m_A is very sensitive to the exact procedure involved in calculating sparticle masses. This results

JHEP03(2002)042

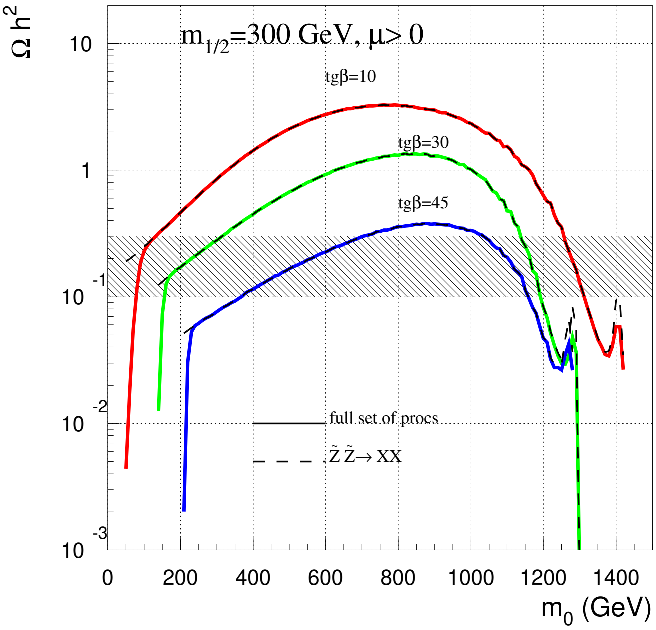

Figure 9: Neutralino relic density $\Omega_{\widetilde{Z}_1}h^2$ versus m_0 for $A_0 = 0$, $m_{1/2} = 300\,\mathrm{GeV}$, $\mu > 0$ and $\tan\beta = 10$, 30 and 45.

in differences in the precise location of the corridor of annihilation through the A and H resonances. Our value of m_A at large $\tan\beta$ seems generally larger than the values obtained in Refs. [26, 23], and somewhat smaller than those obtained in Refs. [29] and [30]. Clearly, more theoretical work needs to be done to stabilize the SUSY and Higgs particle mass predictions at large $\tan\beta$. Finally, the width of the bands of cosmologically favored relic density around the A, H annihilation corridors appears much wider in our results than in the results of refs. [23, 26]. This might be an effect of our improved treatment including *relativistic* thermal averaging. It would be useful to have a comparison against similar results from the group Belanger et al. [34] when these become available.

We presented all our results within the framework of the mSUGRA model. We found four regions of parameter space that led to relic densities in accord with results from cosmological measurements, i.e. $0.1 < \Omega_{\widetilde{Z}_1}h^2 < 0.3$. These include i.) the region dominated by t-channel slepton exchange, ii.) the region dominated by stau co-annihilation, iii.) the large m_0 region dominated by a more higgsino-like neutralino and iv.) the broad regions at high $\tan\beta$ dominated by off-shell annihilation through the A and H Higgs boson resonances. Regions ii) and iii) generally have large fine-tuning associated with them, and although it is logically possible that nature has chosen such parameters, any slight deviation of model parameters would lead to either too low or too high a relic density. Region i) generally has the property that some of the sleptons have masses less than about 300-400 GeV. This region can give rise to a rich set of collider signatures, since many of the sparticles are relatively light.

Region iv) gives broad regions of model parameter space with reasonable values of relic density as well as low values of the fine-tuning parameter. It can also allow quite heavy

JHEP03(2002)042

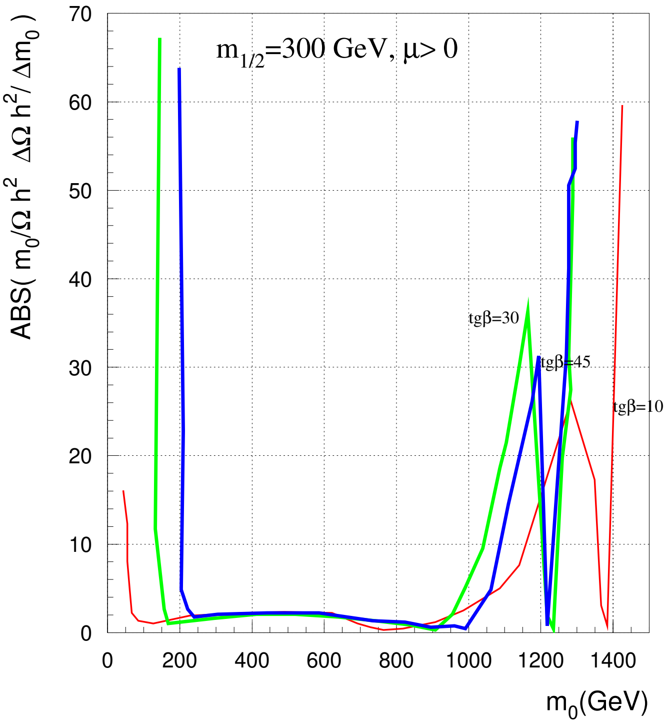

Figure 10: The fine tuning parameter as the function of m_0 for $\tan\beta = 10, 30, 45$ and for the parameter slice $m_{1/2} = 300\,\text{GeV}$, $\mu > 0$.

values of SUSY particle masses, which would be useful to suppress many flavor-violating (such as $b \to s\gamma$) [44] and CP violating loop processes, and the muon $g-2$ value [45]. In many respects region *iv*) is a favored region of parameter space. The neutralino relic density may well point the way to the sort of SUSY signatures we should expect at high energy collider experiments.

Acknowledgments

We thank Manuel Drees, Konstantin Matchev, Leszek Roszkowski and Xerxes Tata for discussions. This research was supported in part by the U.S. Department of Energy under contract number DE-FG02-97ER41022.

References

[1] MAXIMA collaboration, A.T. Lee et al., *A high spatial resolution analysis of the maxima-1 cosmic microwave background anisotropy data*, *Astrophys. J.* **561** (2001) L1 [`astro-ph/0104459`];
Boomerang collaboration, C.B. Netterfield et al., *A measurement by boomerang of multiple peaks in the angular power spectrum of the cosmic microwave background*, `astro-ph/0104460`;
N.W. Halverson et al., *DASI first results: a measurement of the cosmic microwave background angular power spectrum*, `astro-ph/0104489`;

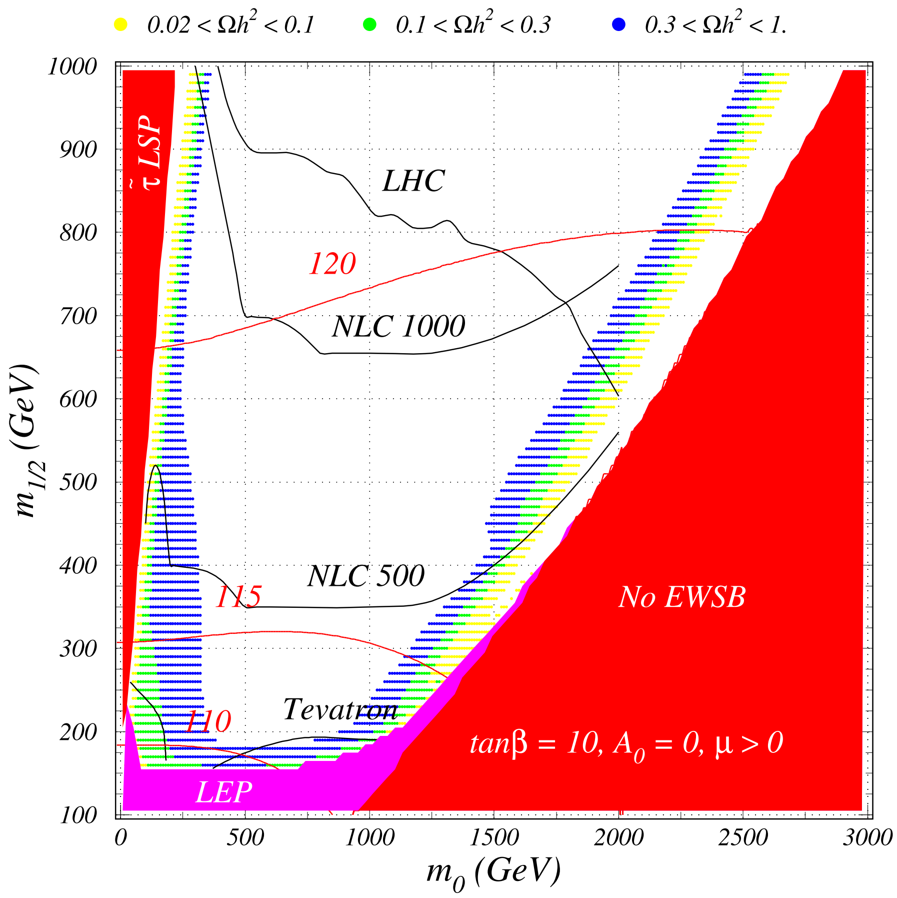

Figure 11: Regions of relic density in the m_0 vs. $m_{1/2}$ plane, including theoretical and experimental constraints, contours of light Higgs mass m_h (red), and reach projections for the Fermilab Tevatron, CERN LHC and Next Linear Collider. We adopt $\tan\beta = 10$, $A_0 = 0$ and $\mu > 0$.

P. de Bernardis et al., *Multiple peaks in the angular power spectrum of the cosmic microwave background: significance and consequences for cosmology*, astro-ph/0105296.

[2] See e.g. W.L. Freedman, *The hubble constant and the expansion age of the universe*, *Phys. Rept.* **333** (2000) 13 [astro-ph/9909076].

[3] Supernova Cosmology Project collaboration, S. Perlmutter et al., *Measurements of omega and lambda from 42 high-redshift supernovae*, *Astrophys. J.* **517** (1999) 565 [astro-ph/9812133].

[4] Boomerang collaboration, A.H. Jaffe et al., *Cosmology from Maxima-1, Boomerang and Cobe/DMR CMB observations*, *Phys. Rev. Lett.* **86** (2001) 3475 [astro-ph/0007333].

[5] K. Olive, G. Steigman and T. Walker, *Primordial nucleosynthesis: theory and observations* *Phys. Rept.* **333** (2000) 389 [astro-ph/9905320];
S. Burles, K.M. Nollett, J.N. Truran and M.S. Turner, *Sharpening the predictions of Big-Bang nucleosynthesis*, *Phys. Rev. Lett.* **82** (1999) 4176 [astro-ph/9901157];
S. Burles, K.M. Nollett and M.S. Turner, *What is the bbn prediction for the baryon density and how reliable is it?*, *Phys. Rev.* **D 63** (2001) 063512 [astro-ph/0008495];

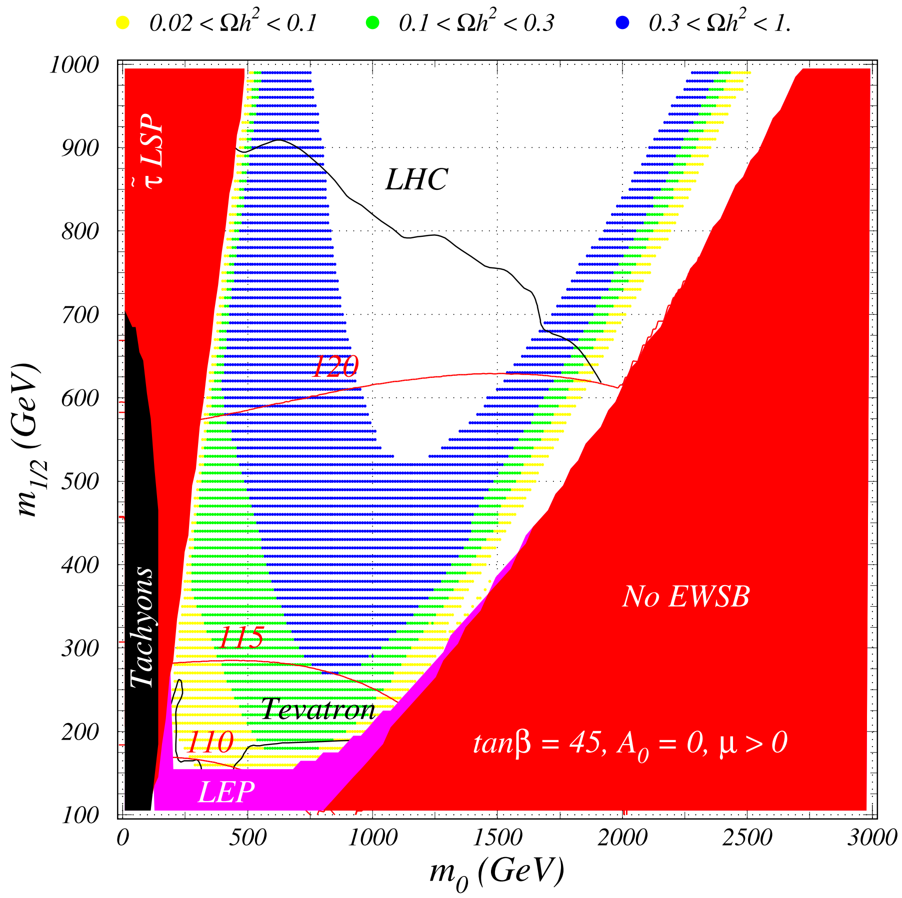

Figure 12: Regions of relic density in the m_0 vs. $m_{1/2}$ plane, including theoretical and experimental constraints, contours of light Higgs mass m_h (red), and reach projections for the Fermilab Tevatron and CERN LHC. We adopt $\tan\beta = 45$, $A_0 = 0$ and $\mu > 0$.

D. Tytler, J. O'Meara, N. Suzuki and D. Lubin, *Review of Big-Bang nucleosynthesis and primordial abundances*, `astro-ph/0001318`.

[6] For a review, see e.g. M. S. Turner, M.S. Turner, *Dark energy and the new cosmology*, `astro-ph/0108103`.

[7] For a review, see G. Jungman, M. Kamionkowski and K. Griest, *Supersymmetric dark matter*, *Phys. Rept.* **267** (1996) 195 [`hep-ph/9506380`].

[8] A.H. Chamseddine, R. Arnowitt and P. Nath, *Locally supersymmetric grand unification*, *Phys. Rev. Lett.* **49** (1982) 970;
R. Barbieri, S. Ferrara and C.A. Savoy, *Gauge models with spontaneously broken local supersymmetry*, *Phys. Lett.* **B 119** (1982) 343;
L.J. Hall, J. Lykken and S. Weinberg, *Supergravity as the messenger of supersymmetry breaking*, *Phys. Rev.* **D 27** (1983) 2359.

[9] H. Baer, F.E. Paige, S.D. Protopopescu and X. Tata, *ISAJET 7.48: a Monte Carlo event generator for pp, $\bar{p}p$ and e^+e^- reactions*, `hep-ph/0001086`.

[10] H. Goldberg, *Constraint on the photino mass from cosmology*, *Phys. Rev. Lett.* **50** (1983) 1419;

J.R. Ellis, J.S. Hagelin, D.V. Nanopoulos and M. Srednicki, *Search for supersymmetry at the $\bar{p}p$ collider*, *Phys. Lett.* **B 127** (1983) 233;
J.R. Ellis, J.S. Hagelin, D.V. Nanopoulos, K.A. Olive and M. Srednicki, *Supersymmetric relics from the Big Bang*, *Nucl. Phys.* **B 238** (1984) 453.

[11] M. Srednicki, R. Watkins and K.A. Olive, *Calculations of relic densities in the early universe*, *Nucl. Phys.* **B 310** (1988) 693.

[12] R. Barbieri, M. Frigeni and G.F. Giudice, *Dark matter neutralinos in supergravity theories*, *Nucl. Phys.* **B 313** (1989) 725.

[13] K. Griest, M. Kamionkowski and M.S. Turner, *Supersymmetric dark matter above the W mass*, *Phys. Rev.* **D 41** (1990) 3565.

[14] K. Griest and D. Seckel, *Three exceptions in the calculation of relic abundances*, *Phys. Rev.* **D 43** (1991) 3191.

[15] P. Gondolo and G. Gelmini, *Cosmic abundances of stable particles: improved analysis*, *Nucl. Phys.* **B 360** (1991) 145.

[16] A. Bottino, V. de Alfaro, N. Fornengo, G. Mignola and S. Scopel, *A new investigation about neutralino dark matter: relic density and detection rates*, *Astropart. Phys.* **1** (1992) 61;
A. Bottino, V. de Alfaro, N. Fornengo, G. Mignola and M. Pignone *On the neutralino as dark matter candidate, 1. Relic abundance*, *Astropart. Phys.* **2** (1994) 67 [hep-ph/9309218];
V. Berezinsky, A. Bottino, J.R. Ellis, N. Fornengo, G. Mignola and S. Scopel, *Neutralino dark matter in supersymmetric models with nonuniversal scalar mass terms*, *Astropart. Phys.* **5** (1996) 1 [hep-ph/9508249].

[17] M. Drees and M.M. Nojiri, *The neutralino relic density in minimal $N = 1$ supergravity*, *Phys. Rev.* **D 47** (1993) 376 [hep-ph/9207234].

[18] J.R. Ellis and L. Roszkowski, *Supergravity dark matter*, *Phys. Lett.* **B 283** (1992) 252;
R.G. Roberts and L. Roszkowski, *Implications for minimal supersymmetry from grand unification and the neutrino relic abundance*, *Phys. Lett.* **B 309** (1993) 329 [hep-ph/9301267];
G.L. Kane, C. Kolda, L. Roszkowski and J.D. Wells, *Study of constrained minimal supersymmetry*, *Phys. Rev.* **D 49** (1994) 6173 [hep-ph/9312272].

[19] P. Nath and R. Arnowitt, *Predictions in* SU(5) *supergravity grand unification with proton stability and relic density constraints*, *Phys. Rev. Lett.* **70** (1993) 3696 [hep-ph/9302318];
R. Arnowitt and P. Nath, *Limits on susy particle spectra from proton stability and dark matter constraints*, *Phys. Lett.* **B 437** (1998) 344 [hep-ph/9801246].

[20] H. Baer and M. Brhlik, *Cosmological relic density from minimal supergravity with implications for collider physics*, *Phys. Rev.* **D 53** (1996) 597 [hep-ph/9508321]; *Neutralino dark matter in minimal supergravity: direct detection vs. collider searches*, *Phys. Rev.* **D 57** (1998) 567 [hep-ph/9706509];
H. Baer et al., *Yukawa unified supersymmetric* SO(10) *model: cosmology, rare decays and collider searches*, *Phys. Rev.* **D 63** (2001) 015007 [hep-ph/0005027].

[21] J. Edsjö and P. Gondolo, *Neutralino relic density including coannihilations*, *Phys. Rev.* **D 56** (1997) 1879 [hep-ph/9704361].

[22] V.D. Barger and C. Kao, *Relic density of neutralino dark matter in supergravity models*, *Phys. Rev.* **D 57** (1998) 3131 [hep-ph/9704403]; *Implications of new CMB data for neutralino dark matter*, *Phys. Lett.* **B 518** (2001) 117 [hep-ph/0106189].

[23] J.R. Ellis, T. Falk, G. Ganis, K.A. Olive and M. Srednicki, *The cmssm parameter space at large* $\tan\beta$, *Phys. Lett.* **B 510** (2001) 236 [hep-ph/0102098].

[24] P. Gondolo, J. Edsjö, L. Bergstrom, P. Ullio and E.A. Baltz, *DarkSUSY: a numerical package for dark matter calculations in the MSSM*, astro-ph/0012234.

[25] J.L. Feng, K.T. Matchev and F. Wilczek, *Neutralino dark matter in focus point supersymmetry*, *Phys. Lett.* **B 482** (2000) 388 [hep-ph/0004043]; *Prospects for indirect detection of neutralino dark matter*, *Phys. Rev.* **D 63** (2001) 045024 [astro-ph/0008115]; *Particle and astroparticle searches for supersymmetry*, hep-ph/0111295.

[26] J.R. Ellis, T. Falk and K.A. Olive, *Neutralino stau coannihilation and the cosmological upper limit on the mass of the lightest supersymmetric particle*, *Phys. Lett.* **B 444** (1998) 367 [hep-ph/9810360];
J. Ellis, T. Falk, K. Olive and M. Srednicki, *Calculations of neutralino-stau coannihilation channels and the cosmologically relevant region of MSSM parameter space*, *Astropart. Phys.* **13** (2000) 181 [hep-ph/9905481], erratum *ibid.* **15** (2001) 414.

[27] R. Arnowitt, B. Dutta and Y. Santoso, *Coannihilation effects in supergravity and D-brane models*, *Nucl. Phys.* **B 606** (2001) 59 [hep-ph/0102181].

[28] M.E. Gomez, G. Lazarides and C. Pallis, *Supersymmetric cold dark matter with Yukawa unification*, *Phys. Rev.* **D 61** (2000) 123512 [hep-ph/9907261];
M.E. Gomez, G. Lazarides and C. Pallis, *Yukawa unification,* $b \to s\gamma$ *and bino stau coannihilation*, *Phys. Lett.* **B 487** (2000) 313 [hep-ph/0004028].

[29] L. Roszkowski, R. Ruiz de Austri and T. Nihei, *New cosmological and experimental constraints on the CMSSM*, *J. High Energy Phys.* **08** (2001) 024 [hep-ph/0106334].

[30] A. Djouadi, M. Drees and J.L. Kneur, *Constraints on the minimal supergravity model and prospects for SUSY particle production at future linear* e^+e^- *colliders*, *J. High Energy Phys.* **08** (2001) 055 [hep-ph/0107316].

[31] C. Boehm, A. Djouadi and M. Drees, *Light scalar top quarks and supersymmetric dark matter*, *Phys. Rev.* **D 62** (2000) 035012 [hep-ph/9911496].

[32] J.R. Ellis, K.A. Olive and Y. Santoso, *Calculations of neutralino stop coannihilation in the CMSSM*, hep-ph/0112113.

[33] A. Pukhov et al., *CompHEP: a package for evaluation of Feynman diagrams and integration over multi-particle phase space. User's manual for version 33*, hep-ph/9908288.

[34] G. Belanger, F. Boudjema, A. Pukhov and A. Semenov, *Micromegas: a program for calculating the relic density in the MSSM*, hep-ph/0112278.

[35] T. Nihei, L. Roszkowski and R. Ruiz de Austri, *Exact cross sections for the neutralino wimp pair-annihilation*, *J. High Energy Phys.* **03** (2002) 031 [hep-ph/0202009].

[36] S. Kawabata, *Monte Carlo integration packages bases and dice*, prepared for *2nd International Workshop on Software Engineering, Artificial Intelligence and Expert Systems for High-energy and Nuclear Physics*, La Londe Les Maures, France, 13-18 Jan 1992.

[37] J.R. Ellis and K.A. Olive, *How finely tuned is supersymmetric dark matter?*, *Phys. Lett.* **B 514** (2001) 114 [hep-ph/0105004].

JHEP03(2002)042

[38] See e.g. ALEPH collaboration, R. Barate et al., *Search for supersymmetric particles in e^+e^- collisions at $\sqrt{s}$ up to 202 GeV and mass limit for the lightest neutralino*, *Phys. Lett.* **B 499** (2001) 67 [hep-ex/0011047].

[39] For combined LEP2 limits on MSSM Higgs bosons, see LEP Higgs Working Group collaboration, *Searches for the neutral Higgs bosons of the MSSM: preliminary combined results using lep data collected at energies up to 209 GeV*, hep-ex/0107030.

[40] H. Baer, M. Drees, F. Paige, P. Quintana and X. Tata, *Trilepton signal for supersymmetry at the Fermilab Tevatron revisited*, *Phys. Rev.* **D 61** (2000) 095007 [hep-ph/9906233]; V.D. Barger and C. Kao, *Trilepton signature of minimal supergravity at the upgraded tevatron*, *Phys. Rev.* **D 60** (1999) 115015 [hep-ph/9811489]; K.T. Matchev and D.M. Pierce, *New backgrounds in trilepton, dilepton and dilepton plus τ jet SUSY signals at the Tevatron*, *Phys. Lett.* **B 467** (1999) 225 [hep-ph/9907505]; for a review, see SUGRA Working Group collaboration, S. Abel et al., *Report of the sugra working group for run II of the Tevatron*, hep-ph/0003154.

[41] J.L. Feng, K.T. Matchev and T. Moroi, *Focus points and naturalness in supersymmetry*, *Phys. Rev.* **D 61** (2000) 075005 [hep-ph/9909334].

[42] H. Baer, C.-h. Chen, F. Paige and X. Tata, *Signals for minimal supergravity at the Cern large hadron collider: multi-jet plus missing energy channel*, *Phys. Rev.* **D 52** (1995) 2746 [hep-ph/9503271]; *Signals for minimal supergravity at the Cern large hadron collider II: multilepton channels*, *Phys. Rev.* **D 53** (1996) 6241 [hep-ph/9512383]; H. Baer, C.-h. Chen, M. Drees, F. Paige and X. Tata, *Probing minimal supergravity at the Cern LHC for large* $\tan\beta$, *Phys. Rev.* **D 59** (1999) 055014 [hep-ph/9809223].

[43] H. Baer, R. Munroe and X. Tata, *Supersymmetry studies at future linear e^+e^- colliders*, *Phys. Rev.* **D 54** (1996) 6735 [hep-ph/9606325], erratum *ibid.* **56** (1997) 4424.

[44] See e.g. H. Baer, M. Brhlik, D. Castano and X. Tata, *$b \to s\gamma$ constraints on the minimal supergravity model with large tan(beta)*, *Phys. Rev.* **D 58** (1998) 015007 [hep-ph/9712305].

[45] See e.g. H. Baer, C. Balazs, J. Ferrandis and X. Tata, *Impact of muon anomalous magnetic moment on supersymmetric models*, *Phys. Rev.* **D 64** (2001) 035004 [hep-ph/0103280].

JHEP03(2002)042